A Structural Approach to Establishing a Platform Chemistry for the Tunable, Bulk Electron Beam Cross-Linking of Shape Memory Polymer Systems

ARTICLE *in* MACROMOLECULES · NOVEMBER 2013

Impact Factor: 5.8 · DOI: 10.1021/ma4018372

8 AUTHORS, INCLUDING:

Keith Hearon
Massachusetts Institute of Technology
17 PUBLICATIONS **192** CITATIONS
SEE PROFILE

Thomas S Wilson
Lawrence Livermore National Laboratory
80 PUBLICATIONS **1,546** CITATIONS
SEE PROFILE

Karen L Wooley
Texas A&M University
327 PUBLICATIONS **17,807** CITATIONS
SEE PROFILE

Duncan John Maitland
Texas A&M University
123 PUBLICATIONS **2,155** CITATIONS
SEE PROFILE

Macromolecules

Article

pubs.acs.org/Macromolecules

A Structural Approach to Establishing a Platform Chemistry for the Tunable, Bulk Electron Beam Cross-Linking of Shape Memory Polymer Systems

Keith Hearon,[†,⊥] Celine J. Besset,[‡] Alexander T. Lonnecker,[‡] Taylor Ware,[§] Walter E. Voit,[§] Thomas S. Wilson,[⊥] Karen L. Wooley,[‡] and Duncan J. Maitland*[,†]

[†]Department of Biomedical Engineering, Texas A&M University, College Station, Texas 77843, United States

[‡]Department of Chemistry, Texas A&M University, College Station, Texas 77842, United States

[§]Department of Materials Science & Engineering, The University of Texas at Dallas, Richardson, Texas 75080, United States

[⊥]Chemical Sciences Division, Physical and Life Sciences Directorate, Lawrence Livermore National Laboratory, Livermore, California 94550, United States

ABSTRACT: The synthetic design and thermomechanical characterization of shape memory polymers (SMPs) built from a new polyurethane chemistry that enables facile, bulk and tunable cross-linking of low-molecular weight thermoplastics by electron beam irradiation is reported in this study. SMPs exhibit stimuli-induced geometry changes and are being proposed for applications in numerous fields. We have previously reported a polyurethane SMP system that exhibits the complex processing capabilities of thermoplastic polymers and the mechanical robustness and tunability of thermomechanical properties that are often characteristic of thermoset materials. These previously reported polyurethanes suffer practically because the thermoplastic molecular weights needed to achieve target cross-link densities severely limit high-throughput thermoplastic processing and because thermally unstable radiation-sensitizing additives must be used to achieve high enough cross-link densities to enable desired tunable shape memory behavior. In this study, we demonstrate the ability to manipulate cross-link density in low-molecular weight aliphatic thermoplastic polyurethane SMPs (M_w as low as ~1.5 kDa) without radiation-sensitizing additives by incorporating specific structural motifs into the thermoplastic polymer side chains that we hypothesized would significantly enhance susceptibility to e-beam cross-linking. A custom diol monomer was first synthesized and then implemented in the synthesis of neat thermoplastic polyurethane SMPs that were irradiated at doses ranging from 1 to 500 kGy. Dynamic mechanical analysis (DMA) demonstrated rubbery moduli to be tailorable between 0.1 and 55 MPa, and both DMA and sol/gel analysis results provided fundamental insight into our hypothesized mechanism of electron beam cross-linking, which enables controllable bulk cross-linking to be achieved in highly processable, low-molecular weight thermoplastic shape memory polymers without sensitizing additives.

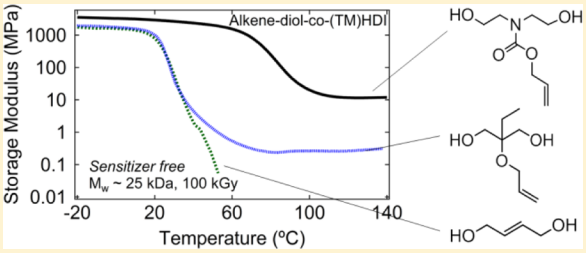

INTRODUCTION

The industrial relevance of polymeric systems is largely dependent on their processability and tailorability of thermomechanical properties. As industrial demands drive innovation in polymer science, processability and tunability of mechanical properties are major factors for consideration during the design stages of polymer development. In particular, for shape memory polymer (SMP) systems, which exhibit stimuli-responsive geometric transformations and have been proposed for numerous engineering and commodity device applications, processability and tailorability of mechanical properties are extremely important material attributes.[1−3] For example, in the aerospace industry, SMP-foam-based actuators for self-deploying aircraft and spacecraft components are being developed, and material properties such as foam modulus and recovery force, in addition to the ability of a polymer to be processed into desired foam geometries, are all crucial design criteria.[4,5] In the medical device industry, proposed neat SMP applications such as interventional embolectomy devices or neurovascular stents also demand tailorability of various material properties and have complex geometric design requirements.[6−11]

The ability of a shape memory polymer system to be processable and to have thermomechanical properties that can be tailored to meet desired design criteria often hinges on the nature of the cross-links in the SMP system. Thermoplastic SMP systems with physical cross-links such as chain entanglements or dispersed glassy or crystalline phases can be processed into desired geometries using thermoplastic processing methods including injection molding or extrusion and consequently have distinct advantages over thermoset SMP systems in the area of processability. However, covalently cross-

Received: September 3, 2013
Revised: October 22, 2013
Published: November 11, 2013

   dx.doi.org/10.1021/ma4018372 | *Macromolecules* 2013, 46, 8905−8916

Scheme 1. In the Study, the Approach is the Synthesis of Polyurethane Shape Memory Polymers with EWG−$CH_{2\alpha}$−C═C Structural Motifs in the Polymer Side Chains To Enhance Susceptibility to Electron Beam Cross-Linking and Eliminate the Need for Sensitizer Additives

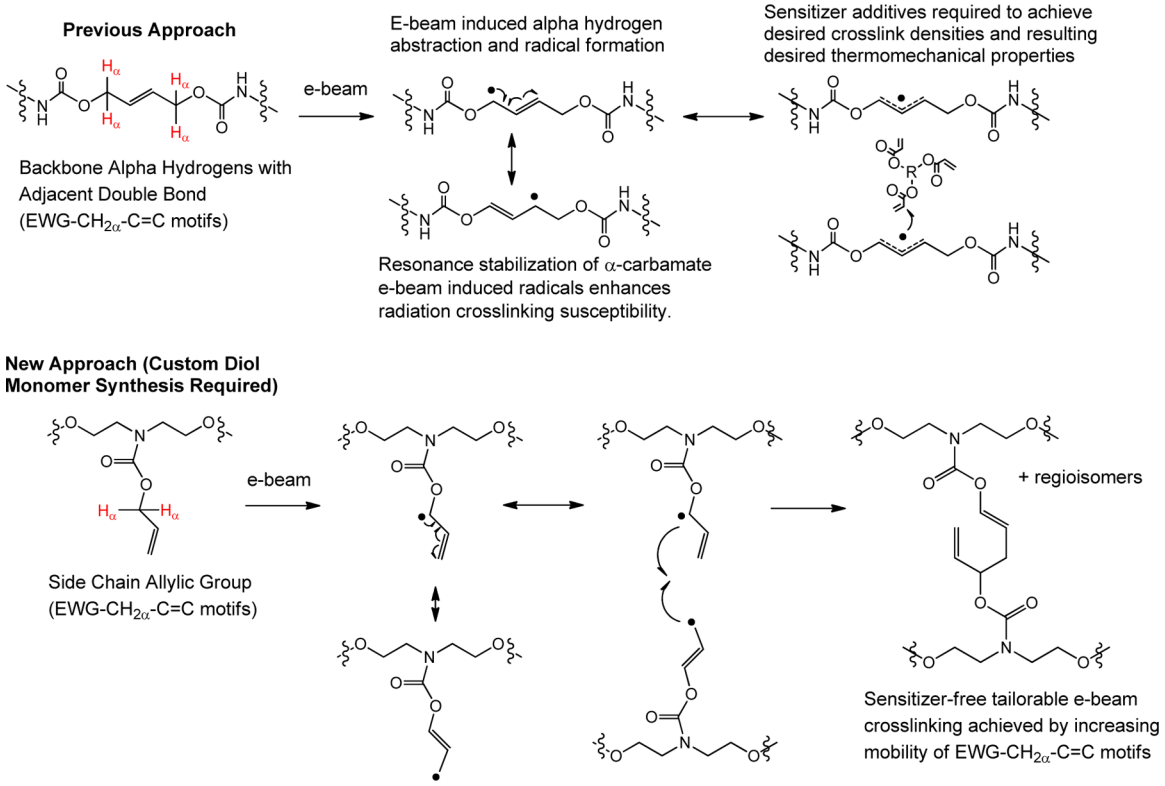

linked SMP systems have often been shown to possess more highly tailorable and generally better shape memory properties than those of certain thermoplastic systems, including higher recovery stress and better cyclic recoverable strain behavior, although advancements in thermoplastic SMP formulation have enabled more robust mechanical behavior for some thermoplastics.[12] For these reasons, an SMP that can be processed into a desired geometry as a thermoplastic and then covalently cross-linked in the bulk state to controllable cross-link densities to allow for tailoring of thermomechanical properties offers advantages for certain industrial applications. Such applications include those requiring the use of high throughput thermoplastic processing techniques or those requiring complex fabrication procedures that must be carried out in atmospheric conditions that also demand the mechanical integrity afforded by a chemistry such as that of polyurethanes, which can be processed in ambient conditions after initial polymerizations in controlled atmospheric environments are carried out. It is also desirable from a thermoplastic processing standpoint for the thermoplastic molecular weight to be low enough to afford rheological behavior favorable for melt processing.[13−16]

The cross-linking of bulk thermoplastic polymers has been achieved in multiple polymeric systems using electron beam irradiation.[17] However, many e-beam cross-linkable thermoplastics suffer practically because high thermoplastic molecular weights, which increase processing difficulty, are often required for e-beam cross-linking to occur,[18] and many of these same thermoplastics also require the addition of reactive sensitizer additives (e.g., polyacrylates) prior to irradiation, which can undergo undesired premature thermally induced reactions during high-temperature processing.[19,20] Additionally, highly cross-linked networks are not commonly reported in e-beam cross-linking studies, which largely define cross-linking in terms of the percentage of polymer chains that are incorporated into a network after irradiation (i.e., gel fraction). For shape memory polymers, it is important that cross-linking also be defined in terms of the number of cross-linking sites that are in a network and that high cross-link densities be achievable if desired, since recovery stress in SMPs is dependent on cross-link density.[21] It is important to note that the penetration depth of electron beam ionizing radiation is generally limited to a maximum of several centimeters in bulk plastic materials (the dual source 10 MeV e-beam accelerator at Texas A&M, which was the irradiation source for all materials in this study, reports a dual penetration of 6.5 cm in media with a density of 1.0 g/cm^3).[22] Consequently, polymeric substrates with significantly greater thicknesses are not suitable for bulk cross-linking by e-beam irradiation.

To improve the overall functional utility of e-beam cross-linkable polymers, it is desirable that cross-linking be achievable in lower molecular weight thermoplastics, that it be attainable without the use of sensitizer additives, and that it be a favorable enough process to afford highly cross-linked networks when desired. We have previously reported that the e-beam cross-linking susceptibility of a polyurethane SMP system can be enhanced by the incorporation of specific structural motifs into the polymer repeat units, as shown in Scheme 1.[23] Although these PU SMPs exhibited high e-beam cross-linking susceptibility in comparison with that of other thermoplastic polymers reported in the literature, acrylic sensitizer additives were still required to achieve cross-link densities in the range of those associated with high recovery stress shape memory materials, with as much as 25 mol % radiation sensitizer being required.[24] In this study, we describe a structural approach to achieving

dx.doi.org/10.1021/ma4018372 | Macromolecules 2013, 46, 8905−8916

Table 1. Monomer Structures and General Thermoplastic Polymer Structures and Illustration of Varying Chemistries Adjacent to C═C Groups in Polymer Backbone or Side Chain[a]

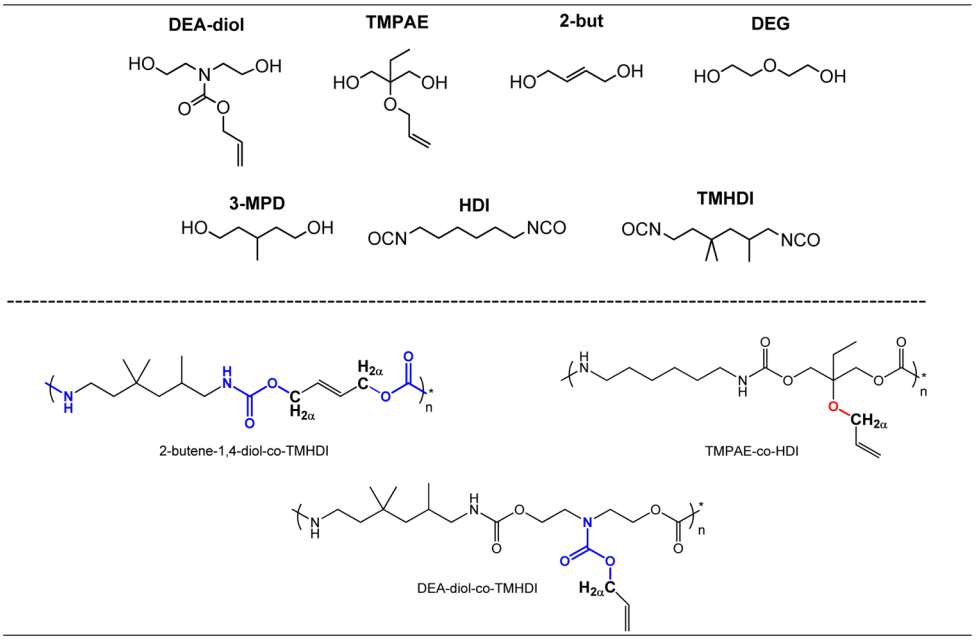

[a]One-pot synthesis of DEA−diol monomer from diethanolamine and allyl chloroformate.

Scheme 2. One-Step Synthesis of DEA-Diol Monomer from Diethanolamine (DEA) and Allyl Chloroformate (ACF)

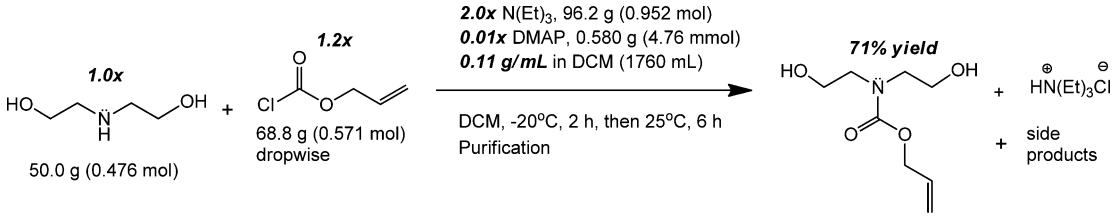

tailorability of cross-link density in a new class of aliphatic, amorphous polyurethane SMPs that undergo e-beam cross-linking as low molecular weight thermoplastics without the use of radiation sensitizers to afford high cross-link densities. As shown in Scheme 1, the α-hydrogen theory of electron beam cross-linking, which has been supported in numerous studies since the 1950s, states that one of the dominant mechanisms of electron beam cross-linking may be the free radical recombination that occurs between e-beam generated radicals after hydrogen atom abstraction at carbons located in positions α to electron withdrawing groups (EWGs) in polymer backbones or side chains.[25−27] We have hypothesized that electron beam cross-linking can be further enhanced by the incorporation of C═C functionalities in positions adjacent to α-EWG C−H units through allylic resonance stabilization of α-EWG C-centered radicals by allowing for longer radical life and therein increasing the probability of cross-linking events occurring by radical recombination. This hypothesis has been supported by others in the literature.[28] Our previously reported PU SMPs were prepared from aliphatic diisocyanates, various saturated aliphatic diols, and 2-butene-1,4-diol, and the resulting general structure of these polymer systems was a backbone EWG−$CH_{2\alpha}$−C═C structural motif.

In the present study, we hypothesize that e-beam cross-linking can be further enhanced by shifting the EWG−$CH_{2\alpha}$−C═C structural motifs from the polyurethane backbones to side chains because of increased mobility of side chain e-beam induced α-carbamate radicals, as illustrated in Scheme 1. Since no alkene diol monomer capable of enabling an EWG−$CH_{2\alpha}$−C═C side chain motif was found to be commercially available, a custom monomer, referred to as "DEA−diol" in this study, was prepared from diethanolamine and allyl chloroformate using a one-pot synthesis and subsequent purification. To compare the effects of side chain electron withdrawing groups on e-beam cross-linking with those of side chain electron donating groups on e-beam cross-linking, an analogue was prepared from the commercially available trimethylolpropane allyl ether (TMPAE) monomer. The radiation cross-linking susceptibility of equivalent molecular weight DEA−diol, TMPAE, and 2-butene-1,4-diol polymers was quantified using sol/gel analysis and dynamic mechanical analysis experiments. The general structures of polymers based on these monomers are provided in Table 1. Other DEA−diol and TMPAE-based polymers with varying C═C content and molecular weights were also synthesized, and the effects of radiation dose, molecular weight, and side chain C═C composition on e-beam cross-linking were quantified using subsequent sol/gel analysis and DMA experiments. The new SMPs were then subjected to multitemperature strain-to-failure experiments and shape memory characterization experiments to determine tensile and shape memory properties.

dx.doi.org/10.1021/ma4018372 | Macromolecules 2013, 46, 8905−8916

MATERIALS AND METHODS

Hexamethylene diisocyanate (HDI), trimethylhexamethylene diisocyanate (TMHDI), 2-butene-1,4-diol (2-but), diethylene glycol (DEG), diethanolamine (DEA), 4-dimethylaminopyridine (DMAP), triethylamine (TEA) and zirconium(IV) acetylacetonate (Zr catalyst) were purchased from TCI America and used as received. Allyl chloroformate (ACF), allyl alcohol (AA), trimethylolpropane allyl ether (TMPAE), and 3-methyl-1,5-pentanediol (3-MPD), and 4 Å molecular sieve beads were purchased from Sigma-Aldrich and used as received. Anhydrous dichloromethane (DCM) and tetrahydrofuran (THF) were purchased from BDH Chemicals and used as received.

Synthesis of the DEA−diol monomer from diethanolamine and allyl chloroformate is depicted in Scheme 2. Diethanolamine (0.476 mol), triethylamine (0.952 mol), and dimethylaminopyridine (4.76 mmol) were dissolved in 1760 mL of anhydrous DCM at 25 °C. The solution was then cooled to −20 °C using a saturated NaCl water bath and stirred vigorously under a dry nitrogen atmosphere. Allyl chloroformate (0.571 mol) was then added dropwise over the course of 2 h. The final reaction mixture had a concentration of 0.11 g/mL in DCM. After 2 h, the solution temperature was allowed to equilibrate at 25 °C and was allowed to stir under dry nitrogen for an additional 6 h. Upon consumption of the starting material, the reaction was quenched by adding the reaction mixture to 1000 mL of ice water. The aqueous layer was extracted with 500 mL (2×) of DCM. The organic layers were combined and washed with aqueous saturated $NaHCO_3$, 0.5 M HCl, and brine. The organic layer was then dried with $MgSO_4$, filtered, and concentrated under reduced pressure. The resulting crude oil was purified by column chromatography with 50% ethyl acetate/50% acetone as an eluent to afford the product as a clear oil (84.4 g, 71% yield). ^{1}H NMR ($CDCl_3$, 500 MHz): δ 5.91−5.78 (dddd, 1H, J = 16.9, 15.5, 5.4, 5.1), 5.25−5.18 (ddd, 1H, J = 17.2 Hz, 3.5, 1.5), 5.16−5.11 (ddd, 1H, J = 10.5, 2.9, 1.5), 4.64 (s, br, 2H, OH) 4.52−4.49 (td, 2H, J = 5.5, 1.5), 3.69 (d, 4H, J = 4.3), 3.39 (t, 4H, J = 4.8) ppm. ^{13}C NMR ($CDCl_3$, 125 MHz): δ 156.6 (C═O), 132.6 (C═C), 117.54 (C═C), 66.2, 61.4, 61.1, 52.4, 51.9 ppm.

Thermoplastic Polyurethane Synthesis. All thermoplastic polyurethanes were synthesized in 33.0 vol % solutions in anhydrous THF. All monomers, solvents, and catalysts were mixed to 100 g scale reaction mixtures under dry air in a LabConco glovebox. Using a 1.01:1.00 NCO:OH ratio, all polymerization reaction products were mixed in the glovebox in 225 mL glass jars that were previously flame-dried, after which the THF and Zr catalyst solution (0.010 wt % catalyst) were added. After adding approximately 80 mL of 4 Å molecular sieves to each polymerization mixture, the polymerizations were carried out in sealed jars using a LabConco RapidVap instrument at 80 °C for 24 h at a vortex setting of 150 rpm. The RapidVap was used to heat and mix the monomer solutions. After 24h, the viscous polymer solutions were filtered to remove molecular sieve dust using flash chromatography and then decanted into 12 in. × 9 in. rectangular polypropylene (PP) dishes, which were placed under vacuum at 80 °C for 72 h to remove solvent.

Polymer film Preparation and Irradiation. To prepare films suitable for DMA and tensile testing experiments, 2 in. × 5 in. × 0.4 mm thick films were prepared by dissolving approximately 5 g of each thermoplastic polymer into 40 mL of THF. The polymer solutions were then redecanted into polypropylene 2 in. × 5 in. × 2 in. polypropylene dishes purchased from McMaster Carr. The THF was allowed to evaporate at ambient pressure at 50 °C for 24 h and then at 80 °C for an additional 24 h using a vacuum oven. The samples were then evacuated at 80 °C at 1 Torr for an additional 24 h and then stored under desiccation until irradiation. The thermoplastic films were irradiated doses varying between 1 and 500 kGy using a 10 MeV electron accelerator located at the Texas A&M University National Center for Electron Beam Research (NCEBR). The dose range of 1−500 kGy was selected because numerous previous studies have demonstrated successful electron beam cross-linking of various polymer systems over this dose range, including our own previous studies. The irradiations were carried out at 40 °C (reported by NCEBR staff) on a conveyor belt, and doses were delivered in 50 kGy/pass increments. Doses were measured using alanine strips, and the uncertainty of dose to product was reported by the NCEBR operators to be 5%. After irradiation, all samples were postcured at 80 °C at 1 Torr for 24 h.

Nuclear Magnetic Resonance Spectroscopy. ^{1}H NMR and ^{13}C NMR spectra were recorded on a Varian Inova 500 spectrometer. Chemical shifts were referenced to the solvent resonance signals.

Molecular Weight Characterization. Gel permeation chromatography (GPC) was performed on a Waters Chromatography, Inc., 1515 isocratic HPLC pump equipped with an inline degasser, a model PD2020 dual angle (15° and 90°), a model 2414 differential refractometer (Waters, Inc.), and four PLgel polystyrene-*co*-divinylbenzene gel columns (Polymer Laboratories, Inc.) connected in series: 5 μm Guard (50 × 7.5 mm), 5 μm MixedC (300 × 7.5 mm), 5 μm 104 (300 × 7.5 mm), and 5 μm 500 Å (300 × 7.5 mm) using the Breeze (version 3.30, Waters, Inc.) software. The instrument was operated at 35 °C with THF as eluent (flow rate set to 1.0 mL/min). Data collection was performed with Precision Acquire 32 Acquisition program (Precision Detectors, Inc.) and analyses were carried out using Discovery32 software (Precision Detectors, Inc.). A system calibration curve generated from plotting molecular weight as a function of retention time for a series of broad polydispersity poly(styrene) standards was used to determine the molecular weight values of polycarbonates, and the value was determined using dn/dc values that were calculated for each sample.

Sol/Gel Analysis. After irradiation and postcuring, dry 50 mg samples irradiated at varying doses and comprised of varying monomer combinations were massed in triplicate and placed in 20 mL glass vials, after which THF was added in approximately a 150:1 solvent:polymer mass ratios. The vials were capped and vortexed at 50 rpm at 50 °C for 48 h using a LabConco RapidVap instrument. After 48 h, the solvent swollen polymer samples were removed from the THF/sol fraction solutions and placed in new 20 mL glass vials, dried at 80 C for an additional 48 h at 1 Torr, and then remassed to provide sufficient mass data to determine the gel fractions of each irradiated sample.

Dynamic Mechanical Analysis. The 4 mm × 30 mm × 0.4 mm rectangular DMA samples were machined using a Gravograph LS100 40 W CO_2 laser machining device. All laser machined samples were sanded around the edges using 400, then 800, then 1200 grit sandpaper. DMA was performed using a TA Instruments Q800 Dynamic Mechanical Analyzer in the DMA Multifrequency/Strain mode in tension using a deformation of 0.1% strain, a frequency of 1 Hz, a force track of 150%, and a preload force of 0.01 N. Each experiment was run from −20 to +140 °C using a heating rate of 2 °C/min.

Differential Scanning Calorimetry. Differential scanning calorimetry (DSC) experiments were run using a TA Instruments Q200 differential scanning calorimeter on 5−10 mg samples. Two-cycle heat−cool-heat experiments were run from 0 to 150 °C using a heating and cooling rate of 20 °C/min. In between heating and cooling cycles, the samples were held isothermally at 0 or 150 °C for 2 min. Only the second-cycle heating data is shown in this publication.

Uniaxial Tensile Testing. ASTM Type V dog bone samples were machined using a Gravograph LS100 40 W CO_2 laser machining device. All laser machined samples were sanded around the edges using 400, then 800, then 1200 grit sandpaper. Strain-to-failure experiments were conducted on select samples ($n \geq 5$) using an Instron Model 5965 electromechanical, screw driven test frame, which was equipped with a 500 N load cell, 1 kN high temperature pneumatic grips, and a temperature chamber that utilizes forced convection heating. An Instron Advanced Video Extensometer with a 60 mm field-of-view lens was used to optically measure the deformation of the samples by tracking parallel lines applied at the ends of the gauge length. The samples were heated to varying desired temperatures under zero load (unclamped bottom grip). The temperature was held at the desired temperature for 30 min to allow for thermal equilibrium to be reached, after which the bottom grip was clamped, and then experiments were started thereafter using a deformation rate of 10 mm/min. Data were recorded using Instron Bluehill 3 software.

Table 2. Compositions and GPC Data for All Samples Synthesized

varying DEA−diol Series	equiv of TMHDI	equiv of DEA−diol	equiv of DEG	equiv of AA	M_n (kDa)	M_w (kDa)	PDI
DEA-0	1.010	0.000	1.000	0.000	2.7	5.0	1.57
DEA-0.1	1.010	0.100	0.900	0.000	2.5	5.2	2.06
DEA-0.5	1.010	0.500	0.500	0.000	3.6	13.5	3.73
DEA-1.0	1.010	1.000	0.000	0.000	3.9	21.5	5.48
varying TMPAE Series	equiv of TMHDI	equiv of TMPAE	equiv of 3-MPD	equiv of AA	M_n (kDa)	M_w (kDa)	PDI
TMPAE-0.1	1.010	0.100	0.890	0.010	15.0	26.9	1.79
TMPAE-0.2	1.010	0.200	0.790	0.010	17.2	30.7	1.79
TMPAE-0.3	1.010	0.300	0.690	0.010	1.9	5.2	2.78
TMPAE-0.5	1.010	0.500	0.490	0.010	1.3	3.7	2.81
TMPAE-0.7	1.010	0.700	0.290	0.010	1.1	3.5	3.01
TMPAE-0.9	1.010	0.900	0.090	0.010	2.8	9.5	2.69
varying AA Series	equiv of HDI	equiv of TMPAE	equiv of diol co-monomer	equiv of AA	M_n (kDa)	M_w (kDa)	PDI
AA-0.01	1.010	0.990	0.000	0.010	73.3	215.0	3.07
AA-0.03	1.010	0.970	0.000	0.030	38.2	76.0	1.99
AA-0.05	1.010	0.950	0.000	0.050	26.7	45.9	1.719
AA-0.10	1.010	0.900	0.000	0.100	15.3	24.2	1.587
2-but-*co*-TMHDI	equiv of TMHDI	equiv of 2-but	equiv of diol co-monomer	equiv of AA	M_n (kDa)	M_w (kDa)	PDI
2-but-0.95	1.010	0.950	0.000	0.050	9.1	25.7	2.82

Shape Memory Characterization. Shape memory characterization experiments were performed using a TA Instruments 800 Dynamic Mechanical Analyzer on the same size 4 mm × 30 mm × 0.4 mm rectangular specimens used for the DMA experiments for select samples. In the DMA strain rate mode in tension, the rectangular specimens were heated to T_g + 25 °C (glass transitions were determined by the peak of the tangent deltas from the previous DMA results), allowed to equilibrate for 30 min, and then strained to deformations of 25% or 50%. The strained samples were then cooled to 0 °C and allowed to equilibrate for an additional 30 min. For constrained recovery experiments, which were used to measure the recovery stress of the materials, the drive force of the DMA instrument was maintained to fix 25% strain, and the samples were heated to 120 °C at 2 °C/min. For free strain recovery experiments, which were used to measure percent recoverable strain, the drive force was set to zero after equilibration at 0 °C, after which 50% prestrained samples were reheated to 80 °C at 2 °C/min as recoverable strain was measured, and upon reaching 80 °C, the samples were cooled back to $T = T_g + 25$ °C, and four more free strain recovery cycles were subsequently carried out to afford a five-cycle experiment. Percent recoverable deformation was recorded using TA Instruments QSeries software.

RESULTS AND DISCUSSION

The objective of this study is the development of a low-molecular weight thermoplastic polyurethane shape memory polymer system that can be cross-linked to tailorable cross-link densities while in the bulk state using electron beam irradiation without the use of radiation sensitizer additives. Such an SMP system is desirable because the combined processability of a thermoplastic SMP and thermomechanical tailorability of a thermoset SMP results in a highly versatile SMP system with a potentially broad application range. To accomplish this objective, a new custom diol monomer predicted to be highly favorable for electron beam cross-linking was synthesized, and the radiation cross-linking susceptibility of polyurethanes prepared from this monomer was quantified and compared to that of polyurethanes made from two other commercially available diol monomers.

The GPC results for all samples synthesized in this study are provided in Table 2. The objective in synthesizing these samples was to quantify the effects of varying chemistry adjacent to C═C motifs, as well as varying dose, molecular weight, and C═C composition on electron beam cross-linking of sensitizer-free polyurethane shape memory polymer samples in order to work toward establishing a platform chemistry to enable facile, tunable, bulk cross-linking of polyurethane shape memory polymers. Since molecular weight has been shown to significantly influence the susceptibility of a polymer to electron beam cross-linking,[29] it was important that equivalent molecular weight samples for DEA−diol, TMPAE, and 2-butene-1,4-diol containing samples be synthesized so that the effects of the adjacent C═C chemistry on e-beam cross-linking could be accurately evaluated. After the series of polymers containing varying DEA−diol composition was synthesized and the M_w of the DEA-1.0 sample was determined to be ∼21.5 kDa, the syntheses of TMPAE and 2-butene-1,4-diol based polymers of similar molecular weights were attempted. To accomplish this objective, varying amounts of the capping agent allyl alcohol (AA) were added to the polymerization mixtures of TMPAE and 2-but based polymers to control molecular weight. Allyl alcohol was selected for the purpose of creating polymer chain ends with the potential for incorporation into the cross-linked networks after irradiation to minimize the number of dangling chain ends and maximize toughness.[30] For TMPAE-based polymers, molecular weight decreased from ∼215 to ∼24 kDa as AA composition increased from 1 to 10 mol %. For 2-butene-1,4-diol based polymers, which have been the focus of multiple previous studies, the 5% AA formulation has been previously shown to give an M_w in the range of 20−25 kDa, and the 2-butene-1,4-diol based polymer synthesized in this study was determined to have an M_w of roughly 25.7 kDa.

The susceptibility of the polymers in Table 2 to electron beam cross-linking was quantified using sol/gel analysis and dynamic mechanical analysis. The random radiation cross-linking of thermoplastic polymers is described by the classical Charlesby−Pinner equation, eq 1[29]

$$s + s^{1/2} = \frac{p_o}{q_o} + \frac{1}{q_0 \mu_1 d} \quad (1)$$

where s is sol fraction, p_0 is degradation density, q_0 is cross-linking density, μ_1 is initial molecular weight (M_n), and d is radiation dose. E-beam irradiation causes both random chain scission and random interchain bond formation (*i.e.*, cross-

dx.doi.org/10.1021/ma4018372 | Macromolecules 2013, 46, 8905−8916

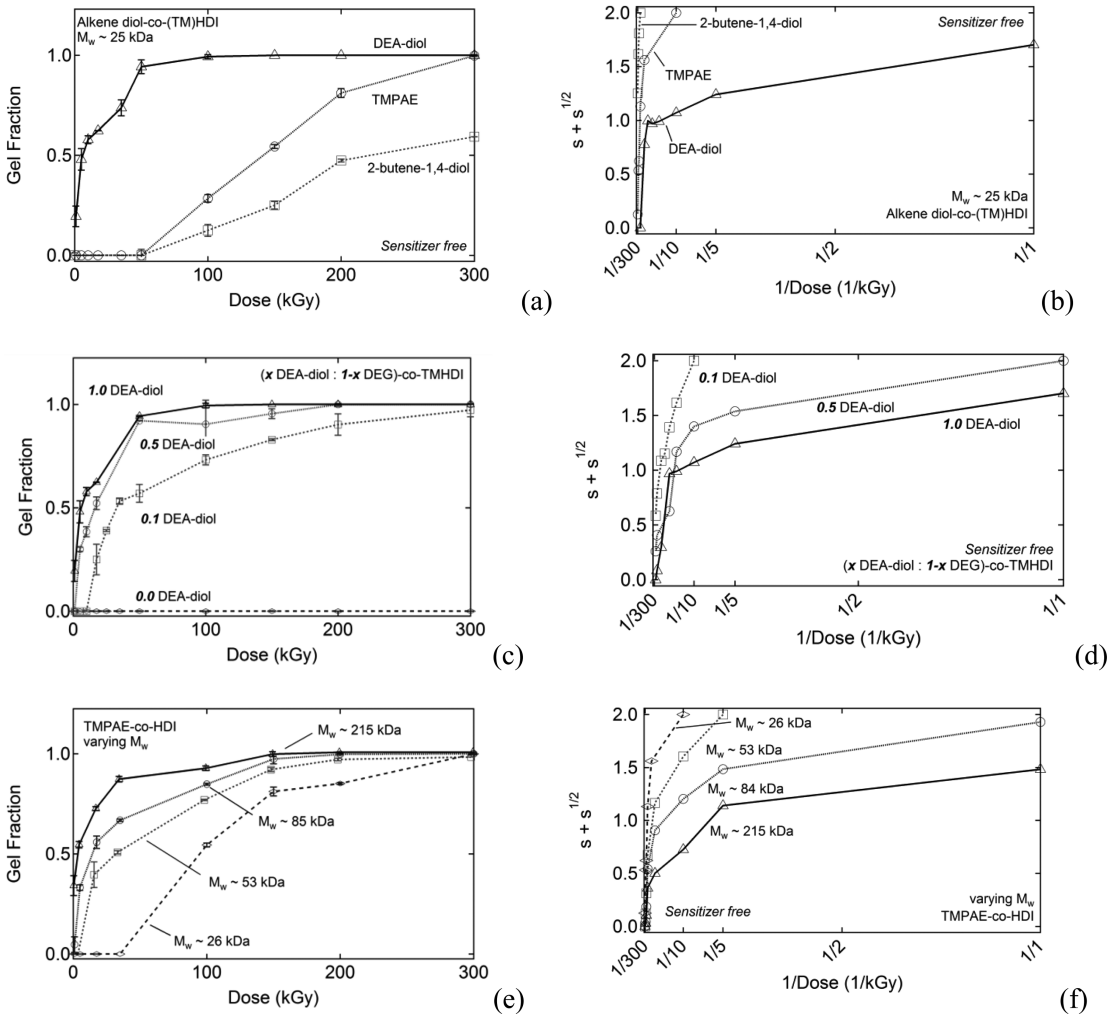

Figure 1. (a) Plots of gel fraction versus dose as determined by sol/gel analysis for polyurethane samples with M_w's of approximately 25 kDa: DEA−diol-*co*-TMHDI (−EWG−$CH_{2\alpha}$−C═C motif in polymer side chain), TMPAE-*co*-HDI (-EDG-$CH_{2\alpha}$−C═C motif in polymer side chain), and 2-but-*co*-TMHDI (−EWG−$CH_{2\alpha}$−C═C motif in polymer backbone). (b) Charlesby−Pinner analysis plots of $s + s^{1/2}$ versus 1/dose for the gel fraction data in part a, where s is sol fraction; (c) plots of gel fraction versus dose for samples containing varying DEA−diol composition; (d) Charlesby−Pinner analysis plots of $s + s^{1/2}$ versus 1/dose for the gel fraction data in part c; (e) plots of gel fraction versus dose for TMPAE-*co*-HDI samples with varying molecular weight; (f) Charlesby−Pinner analysis plots of $s + s^{1/2}$ versus 1/dose for the gel fraction data in part e.

Table 3. Charlesby−Pinner Parameters Calculated for Irradiated PU's Made from Varying Alkene Diols, Varying Alkene Diol Composition, and Varying Molecular Weight

description	sample	d_0	p_0/q_0	R^2
varying C═C composition	DEA-0.10	10.96	0.695	0.929
	DEA-0.50	1.13	0.709	0.709
	DEA-1.00	0.88	0.620	0.466
varying M_w	AA-0.10	10.92	0.635	0.639
	AA-0.05	5.68	0.373	0.373
	AA-0.03	1.08	0.516	0.588
	AA-0.01	0.77	0.324	0.324
varying adjacent chemistry to C═C groups	2-but-0.95 (2-but)	106.73	1.000	0.896
	AA-0.10 (TMPAE)	10.91	0.630	0.639
	DEA-1.00 (DEA−diol)	0.88	0.640	0.490

linking), and the ratio of scission to cross-linking, p_0/q_0, represents the inverse cross-linking efficiency of a polymer system at a specific dose. In a classical Charlesby−Pinner analysis plot, $s + s^{1/2}$ is plotted against $1/d$, and a linear fit of the data yields a positively sloping trend line with intercepts at $s + s^{1/2}$ equals 2 and $1/d$ equals 0. The $s + s^{1/2}$ equals two intercept represents the inverse cross-linking efficiency, represented by p_0/q_0, and the $1/d$ equals 0 intercept represents d_0, the minimum dose to gelation, which is a calculated parameter that represents the theoretical dose required to achieve cross-linking in 1% of a polymer's chains.[31] A polymer that is highly susceptible to electron beam cross-linking has a low d_0, while a

dx.doi.org/10.1021/ma4018372 | *Macromolecules* 2013, 46, 8905−8916

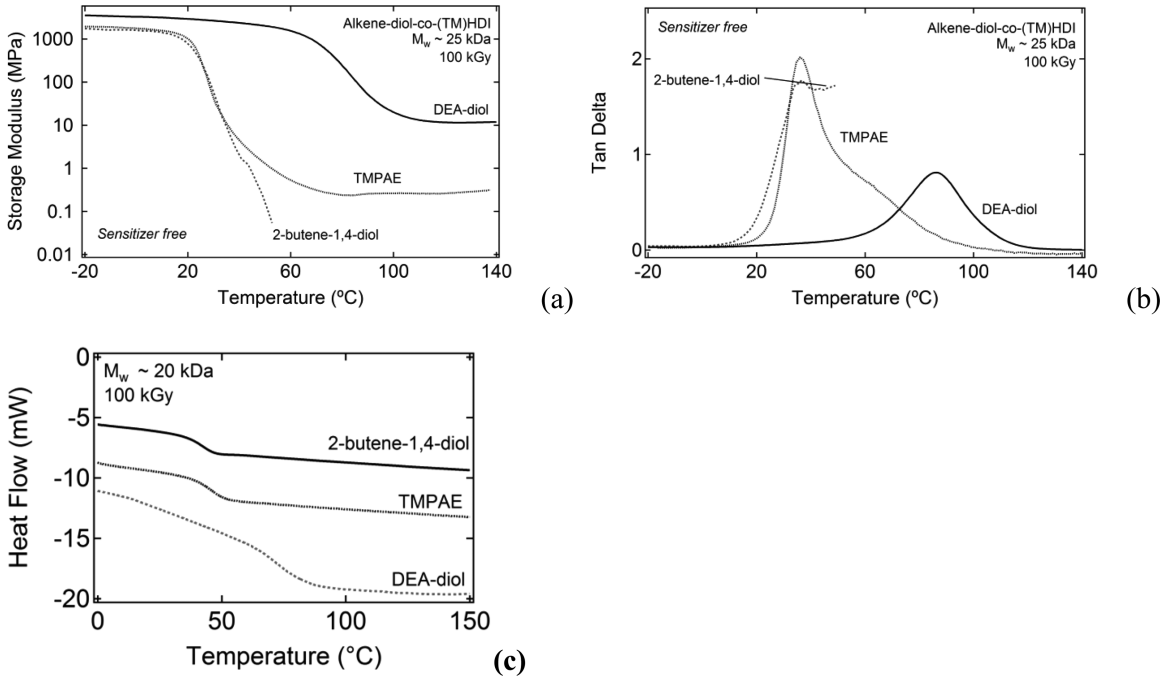

Figure 2. (a) Plots of storage modulus versus temperature as determined by DMA for polyurethane samples with M_w's of approximately 25 kDa: DEA−diol-*co*-TMHDI (−EWG−$CH_{2\alpha}$−C═C motif in polymer side chain), TMPAE-*co*-HDI (−EDG−$CH_{2\alpha}$−C═C motif in polymer side chain), and 2-but-*co*-TMHDI (−EWG−$CH_{2\alpha}$−C═C motif in polymer backbone); (b) plots of tangent delta versus temperature as determined by DMA for the samples whose storage modulus data are provided in part a; (c) DSC thermograms for the same 2-but, TMPAE, and DEA−diol samples with M_w's in the range of 25 kDa irradiated at 100 kGy.

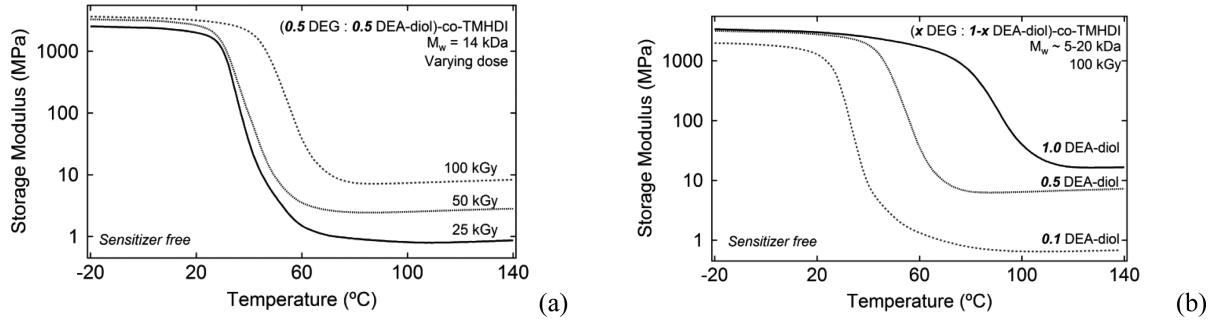

Figure 3. DMA results tailoring rubbery modulus, DEA−diol: (a) varying dose; (b) varying DEA−diol;.

polymer that is not favorable for electron beam cross-linking has a high d_0. D_0 has been shown in previous studies to decrease with increasing molecular weight,[24,29] and one of the objectives in this study is to determine the extent to which d_0 is dependent on adjacent C═C chemistry (*i.e.*, backbone vs. side chain C═C position and adjacent C═C EWG's vs. adjacent C═C EDG's).

Sol/gel analysis plots of gel fraction versus dose for the irradiated polymer samples in Table 1 are provided in Figure 1, parts a, c, and e, Charlesby−Pinner analysis plots of $s + s^{1/2}$ versus $1/d$ for each respective gel fraction plot are provided in Figure 1, parts b, d, and f, and calculated Charleby−Pinner parameters are provided in Table 3. Parts a and b of Figure 1 demonstrate that, for polymer samples with M_w's in the range of 20−25 kDa, DEA−diol-based polymers are the most susceptible to e-beam cross-linking, TMPAE-based polymers are the second-most susceptible, and 2-butene-1,4-diol polymers are the least susceptible. The calculated d_0 values provided in Table 3 profoundly demonstrate the differences in e-beam cross-linking susceptibility for these polymers. D_0 increases roughly an order of magnitude, from 0.88 to 10.91 to 106.73 kGy, as the polymer repeat unit chemistry changes from side chain EWG−$CH_{2\alpha}$−C═C (DEA−diol) to side chain EDG−$CH_{2\alpha}$−C═C (TMPAE) to backbone EWG−$CH_{2\alpha}$−C═C (2-butene-1,4-diol) chemistry. The linearity of the Charlesby−Pinner plots in Figure 1(b) is greatest for 2-butene-1,4-diol, second greatest for TMPAE, and lowest for DEA−diol polymers, as indicated by the R^2 values in Table 3, which decrease from 0.896 to 0.639 to 0.490, respectively. Deviation from linearity in a Charlesby−Pinner plot indicates that cross-linking events are occurring in a less random and more directed manner, and previous studies have shown that adding sensitizer to thermoplastic polymer blends results in deviations from linearity that are similar to those observed in Table 3.[24,32] In this study, the DEA−diol chemistry (and to a lesser degree the TMPAE and 2-butene-1,4-diol chemistries) effectively act as in-chain sensitizers. The gel fraction versus dose trends in Figure 1, parts c and d, show that radiation cross-linking susceptibility increases with increasing C═C composition for DEA−diol copolymers, and the gel fraction versus

dx.doi.org/10.1021/ma4018372 | *Macromolecules* 2013, 46, 8905−8916

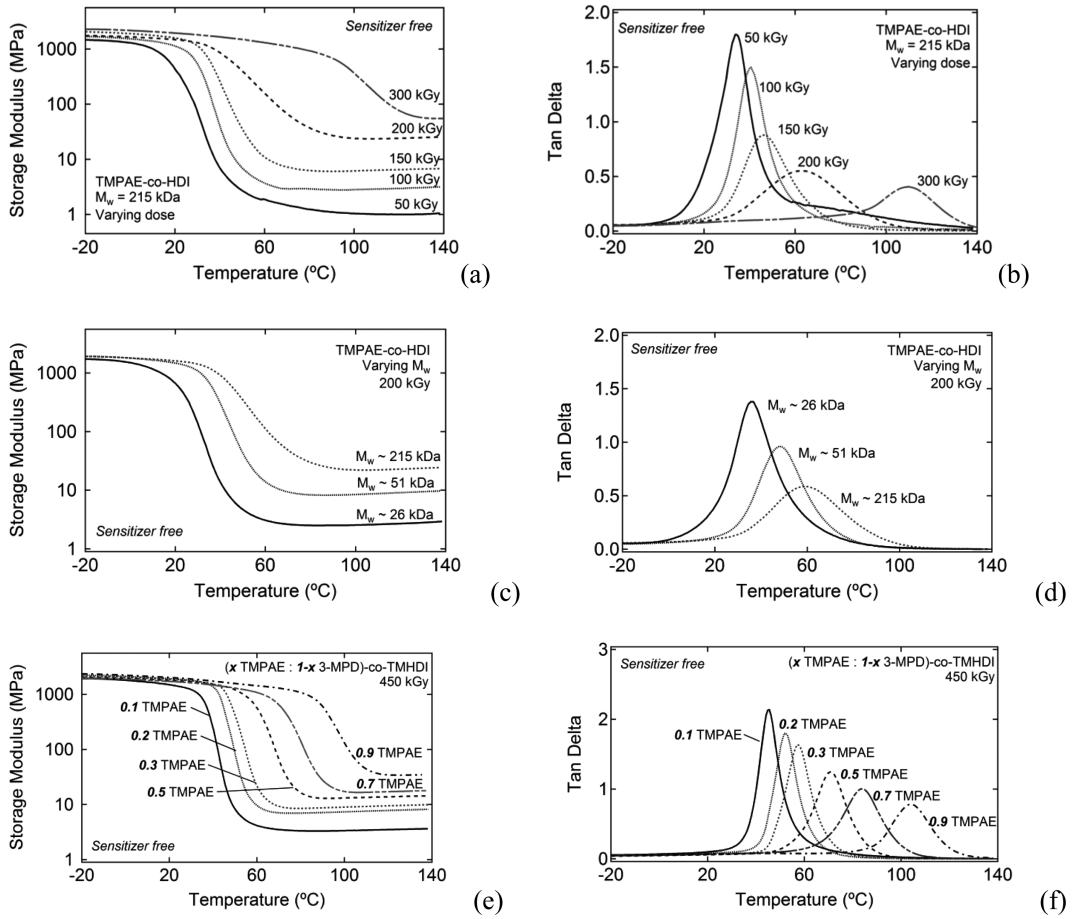

Figure 4. Storage modulus and corresponding tan delta plots for TMPAE-containing samples that demonstrate that cross-link density can be moved over a significant range by varying dose (a, b), molecular weight (c, d), and side chain C═C composition (e, f).

dose trends in Figure 1, parts e and f, show that radiation cross-linking susceptibility increases with increasing M_w for TMPAE copolymers. Both these results are consistent with those for 2-butene-1,4-diol based copolymers reported in previous studies.

The DMA results in Figures 2−4 demonstrate that trends in cross-link density for irradiated samples follow the same trends as those of gel fraction. Parts a and b of Figure 2 contain plots of storage modulus and tangent delta, respectively, versus temperature for the M_w ~ 20−25 kDa DEA−diol, TMPAE, and 2-but samples irradiated at 100 kGy. Rubbery modulus, E_r, defined by the equation of an ideal rubber to be inversely proportional to the average molecular weight between cross-link sites, is greatest for DEA−diol polymer (~15 MPa) and significantly lower for TMPAE polymer (~0.5 MPa).[33,34] The 2-butene-1,4-diol polymer does not have a rubbery plateau regime after irradiation at 100 kGy and, therefore, does not exhibit thermomechanical behavior characteristic of that of a covalently cross-linked polymer (*i.e.*, a glassy modulus plateau at temperatures below its glass transition, a transition region in which modulus decreases with increasing temperature, and a rubbery plateau region in which modulus increases linearly with increasing temperature).[35] When the d_0 values in Table 3 are combined with the storage modulus data in Figure 2(a), the calculated order-of-magnitude variations appear consistent with the observed DMA data. The 2-butene-1,4-diol sample was determined to have a d_0 of 106.73 kGy, which indicates that, upon irradiation at 106.73 kGy, roughly 1% of this polymer's chains should be incorporated into a network. The lack of a rubbery plateau modulus altogether for this sample in Figure 2(a), which shows plots of storage modulus versus temperature for samples irradiated at 100 kGy, is consistent with a d_0 of 106.73 kGy. The significant increases in rubbery modulus for TMPAE and then for DEA−diol samples, respectively also support the calculated d_0 values for these samples in Table 3. DSC results for these three polymers are also provided in Figure 2(c) and indicate that all three samples are amorphous.

Parts a and b of Figure 3 demonstrate that cross-link density increases with increasing dose and increasing C═C composition, respectively, for DEA−diol based polymers. Figure 3a shows that increasing the dose for the DEA-0.5 sample from 25 to 100 kGy results in an increase in rubbery modulus from ~0.9 to ~10.1 MPa. Figure 3b shows that increasing DEA−diol composition from 0.1 diol mole fraction to 1.0 diol mole fraction results in an increase in rubbery modulus from ~0.4 to 15 MPa for samples irradiated at 100 kGy. Similar trends are shown for TMPAE-based polymers in Figure 4. Figure 4a demonstrates that for a 215 kDaA M_w TMPAE-*co*-HDI sample, rubbery modulus increases from 1.1 to 55.0 MPa as dose is increased from 50 to 300 kGy. Figure 4c demonstrates that, for TMPAE-*co*-HDI samples with varying M_w irradiated at 200 kGy, rubbery modulus increases from 2.1 to 22.4 MPa as M_w increases from 26 to 215 kDa. Figure 4e demonstrates that rubbery modulus increases from 3.1 to 33.5 MPa as TMPAE composition increases from 0.1 diol mole fraction to 0.9 diol mole fraction for samples irradiated at 450 kGy. A high dose (450 kGy) for the samples in Figure 4e was necessary to

dx.doi.org/10.1021/ma4018372 | *Macromolecules* 2013, 46, 8905−8916

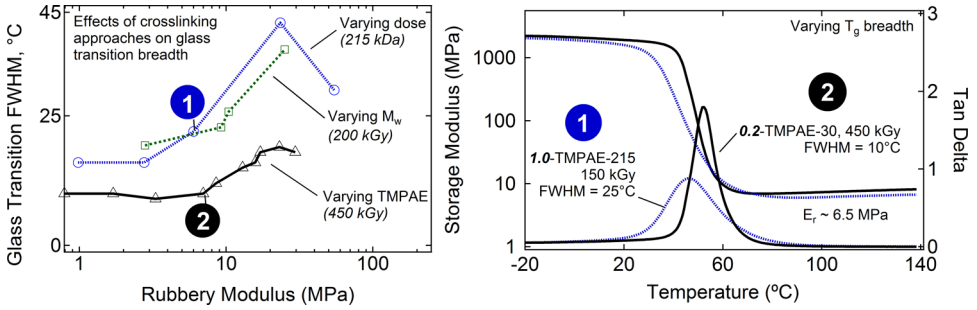

Figure 5. (a) Plots of glass transition breadth as determined by tangent delta full width half-maximum values (fwhm) versus rubbery modulus for the three series of samples shown in Figure 4, in which cross-link density is controlled by varying dose, varying molecular weight, and by varying TMPAE composition; (b) plots of storage modulus and tan δ corresponding to points 1 and 2 in part a, which show near equivalent rubbery modulus values of ~6.5 MPa but glass transition breadths of approximately 25 °C for composition 1 and 10 °C for composition 2.

achieve desirable cross-linking for this low molecular weight series of samples. The plots of tangent delta versus temperature in Figure 4, parts b, d, and f, generally follow similar trends: namely, glass transition increases with increasing cross-link density, as can be seen by the corresponding plots of storage modulus versus temperature. For SMP systems, the ability to control glass transition is an important aspect of the material design process, and certain applications may require that T_g be controllable in a manner that is independent or semi-independent of cross-link density. While this work focuses on achieving control of cross-link density in a new e-beam cross-linkable PU SMP system, future efforts will focus on controlling glass transition.

One notable attribute of the storage modulus and tangent delta data in Figure 4 is the variation in glass transition breadths that are observed for the three methods of controlling cross-link density. The more narrow the breadth of the glass transition in an SMP, the more precise the shape actuation will be with respect to actuation at a specific temperature, and the more rapid the shape recovery time will be.[36] One common method of quantifying the breadth of glass transitions in polymers is to measure the tan delta peak full width half-maximum values, which correspond to the temperature range that spans from one tan delta peak half-maximum value to the other, and SMPs with high network homogeneity generally exhibit narrow T_g breadths. Figure 5a shows plots of glass transition breadth, fwhm (°C) versus rubbery modulus for the three series of SMPs whose DMA data are provided in Figure 4. For all three series, T_g breadth generally increases with increasing rubbery modulus, although several points should be noted. First, for the varying TMPAE series, T_g breadth only varies over a fwhm range of 10−19 °C, while that of the varying dose and varying M_w series varies over larger ranges of 16 to 43 °C and 21 to 39 °C, respectively. One possible explanation for this behavior is that, since both the varying dose and varying molecular weight series are comprised of 1.0 TMPAE diol fractions and possess a maximum number of cross-linking sites for this SMP system, the materials in these series may be able to undergo cross-linking at lower irradiation doses given their high TMPAE composition, while the materials in the varying TMPAE series, which possess fewer cross-linking sites and have lower molecular weights in most cases, must be subjected to higher doses to enable cross-linking. It is possible that irradiation at high doses (450 kGy) in the varying TMPAE series results in a high percentage of the TMPAE cross-linking sites' undergoing cross-linking and affords networks with high degrees of homogeneity. If this same reasoning is applied to the varying dose and varying M_w series, the argument could be made that the materials in this series are susceptible enough to e-beam cross-linking such that some, but not all, of their cross-linking sites undergo e-beam cross-linking, and this "partial" cross-linking could increase network heterogeneity and broaden glass transitions. This argument is supported by the fact that the T_g breadth of the varying dose series decreases from 43 to 30 °C as dose increases from 200 to 300 kGy, even though rubbery modulus also increases from 23.4 to 54.5 MPa. A key concept to take away from the glass transition breadth trends shown in Figure 5 is that, if a specific rubbery modulus value is desirable for an SMP from this series, although multiple methods of achieving this rubbery modulus value may be viable, it appears that keeping TMPAE (or an alternative C═C containing monomer) functionality to a minimum value and irradiating at sufficient dose to cause the majority of the cross-linkable sites to become incorporated in the polymer network may be the best synthetic approach to achieving narrow glass transitions. Figure 5b, which shows plots of storage modulus and tan delta versus temperature for a 1.0 TMPAE sample irradiated at 150 kGy (point 1 in Figure 5a) and a 0.2 TMPAE sample irradiated at 450 kGy (point 2 in Figure 5a), illustrates this concept. While both samples exhibit rubbery moduli of approximately 6.5 MPa, the T_g fwhm value for the 1.0 TMPAE, 150 kGy sample is 25 °C, while that of the 0.2 TMPAE, 50 kGy sample is 10 °C.

To provide a general indication of the performance that can be expected from this new SMP system over a temperature range representative of that which an SMP used in medical device applications could be subjected and to demonstrate that high radiation dose does not result in decreased mechanical integrity as shown in some polymer systems,[37] strain-to-failure experiments for TMPAE-0.1 samples irradiated at 450 kGy were conducted at temperatures ranging from 0 to 65 °C and are provided in Figure 6 along with calculated average toughness values for each straining temperature. The temperatures selected for the strain-to-failure experiments were 65 °C (T_g + 20 °C), 45 °C (T_g), 35 °C (T_g − 10 °C), 20 °C (T_g − 25 °C), and 0 °C (T_g − 45 °C), where T_g was defined by the tangent delta peak temperature as determined by DMA. The stress−strain behavior at each temperature is consistent with that of typical temperature-dependent polymeric behavior.[38] While good mechanical integrity is generally predicted for lightly cross-linked polyurethanes, it is important to demonstrate that good mechanical integrity is still exhibited by materials in this SMP system after subjection to high doses. Average toughness values of 59.3 ± 2.8 and 45.6 ± 3.2 MJ/m^3

dx.doi.org/10.1021/ma4018372 | Macromolecules 2013, 46, 8905−8916

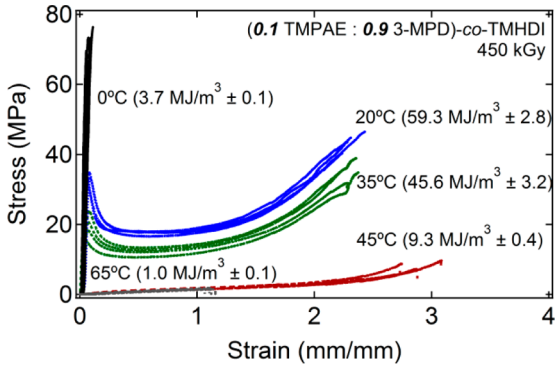

Figure 6. Strain-to-failure at various temperatures for 0.1 TMPAE SMP irradiated at 450 kGy. Average toughness values are provided in parentheses next to each straining temperature and ranged from 1.0 ± 0.1 MJ/m^3 at 65 °C to 59.3 ± 2.8 MJ/m^3 at 20 °C.

were observed at 20 and 35 °C, respectively, and consequently the strain-to-failure results demonstrate that good mechanical integrity can be maintained upon high dose irradiation over a temperature range that is relevant for medical device applications.

The shape memory characterization data provided in Figure 7 demonstrate that the polymers synthesized in this study exhibit good shape memory behavior. The free strain recovery data in parts a and b of Figure 7 show five-cycle thermomechanical cycling for 0.50 mm/mm prestrain for a 0.1 TMPAE, 450 kGy SMP in (a) strain-temperature and (b) strain-time and stress-time planes. As noted in Figure 7a, the recoverable strain, ε_{rec}, was 90% for cycle 1 and was greater than 99% for cycles 2−5. Covalent cross-linking is expected to result in good cyclic shape recovery for SMPs, and parts a and b of Figure 7 demonstrate such behavior.[36] The constrained recovery data in Figure 7c shows increasing recovery stress for TMPAE samples with increasing cross-link density under 25% constrained deformation conditions. Recovery stress increases from 0.5 to 3.0 MPa at tangent delta peak temperature +25 °C as rubbery modulus increases from 3.1 to 15.2 MPa (TMPAE-0.1 to TMPAE-0.7, 450 kGy). Achieving tailorable recovery stress through the control of cross-link density using e-beam irradiation in low molecular weight thermoplastics without the use of sensitizer was one of the underlying motivations in designing the SMP system in this study, and Figure 7c demonstrates the successful achievement of this objective in for thermoplastics with initial molecular weights of 26.9, 5.2, 3.7, and 3.5 kDa.

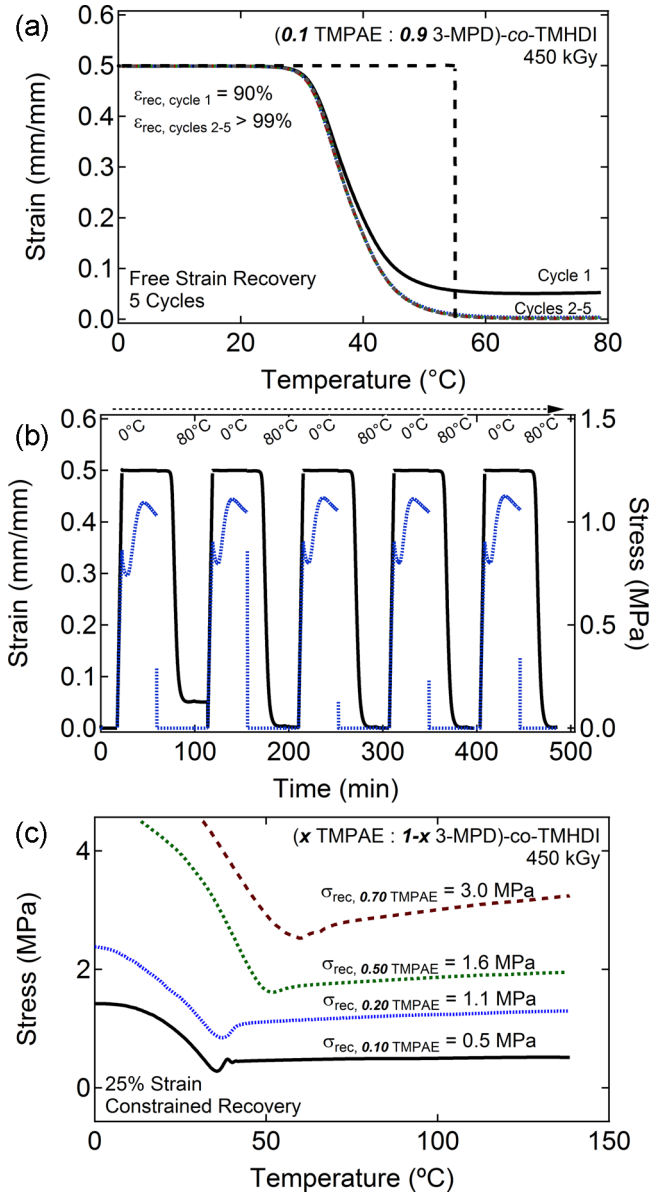

Figure 7. Five-cycle free strain recovery data for a 0.1 TMPAE, 450 kGy SMP subjected to 0.50 mm/mm prestrain shown in (a) strain-temperature and (b) strain-time and stress-time planes. For cycle 1, 90% recoverable strain was observed, and for cycles 2−5, greater than 99% recoverable strain was observed. (c) Constrained recovery analysis showing increased recovery stress with increasing rubbery modulus for electron beam cross-linked SMPs comprised of varying TMPAE composition irradiated at 450 kGy.

CONCLUSIONS

A structural approach to achieving both facile processability and significant tunability of thermomechanical properties in a versatile aliphatic polyurethane shape memory polymer system is reported in this study. The effects of varying chemistry adjacent to C═C motifs, as well as varying dose, molecular weight, and C═C composition on electron beam cross-linking of sensitizer-free polyurethane shape memory polymers are determined in order to work toward establishing a platform chemistry to enable facile, tunable, bulk cross-linking of polyurethane shape memory polymers. As hypothesized, incorporation of EWG−$CH_{2\alpha}$−C═C motifs into the side chains of thermoplastic polyurethane SMPs, which was achieved by synthesizing the custom monomer DEA−diol, results in higher susceptibility to electron beam cross-linking than that which results from incorporating the TMPAE monomer's EDG−-$CH_{2\alpha}$−C═C side chain motifs or the 2-butene-1,4-diol monomer's EWG−$CH_{2\alpha}$−C═C backbone motifs. However, SMPs containing the commercially available TMPAE monomer's EDG−$CH_{2\alpha}$−C═C side chain motifs were also shown to provide sufficient e-beam cross-linking susceptibility to enable control of shape memory properties over a notable range, with rubbery modulus being tailorable between 1 and 55 MPa. The cross-link density of the TMPAE-based SMPs was demonstrated to be tunable by varying dose, molecular weight, and/or C═C monomer composition. Consequently, the thermomechanical properties of this SMP system can be achieved by multiple routes, and the SMP system

dx.doi.org/10.1021/ma4018372 | Macromolecules 2013, 46, 8905−8916

appears to be quite versatile. On the basis of the observed trends in glass transition breadth for the cross-linked SMPs in this study, the combination of minimizing C═C monomer functionality and irradiating at sufficient dose to drive cross-linking reactions to occur in a high percentage of whatever number of cross-linkable sites are necessary to achieve a desirable rubbery modulus appears to afford glass transition breadths that generally remain more narrow as cross-link density is increased than those that are afforded by higher C═C functionalized thermoplastics that are more susceptible to partial cross-linking at lower doses.

The ability to achieve tunable, bulk cross-linking in thermoplastics using the synthetic strategy hypothesized and supported herein may be of interest in a number of industrial applications outside the field of SMP research because the incorporation of even a small amount of the chemical functionalities in this study can be used to greatly influence and improve the resulting mechanical properties of a material system. Since tailorable cross-linking is achievable even for low molecular weight thermoplastics without sensitizer, these SMP materials may be very well-suited for high throughput thermoplastic melt processing techniques. The advanced processing capability and demonstrated tunability of material properties in this SMP system may enable a wide range of applications in biomedical engineering and other industries. Potential high-impact applications range in complexity from 3D printable tissue scaffolds with tailorable moduli possessing shape memory properties to shape memory catheters used in basic medical procedures that must be produced on a mass-scale to justify production costs. Future work will focus on the rheological characterization, complex fabrication and further thermomechanical optimization of this new polyurethane SMP system, including in-depth shape memory characterization and new synthetic strategies to achieving tunable glass transitions.

■ AUTHOR INFORMATION

Corresponding Author

*E-mail: (D.J.M.) djmaitland@tamu.edu.

Author Contributions

The manuscript was written through contributions of all authors. All authors have given approval to the final version of the manuscript.

Notes

The authors declare no competing financial interest.

■ ACKNOWLEDGMENTS

This work was partially performed under the auspices of the U.S. Department of Energy by Lawrence Livermore National Laboratory under Contract DE-AC52-07NA27344. This material is also based upon work supported by the National Science Foundation Graduate Research Fellowship No. 1114211 and No. 2011113646 and by National Institutes of Health/National Institute of Biomedical Imaging and Bioengineering Grant R01EB000462. The authors also acknowledge financial support from the National Science Foundation (CHE-1057441) and the Welch Foundation W. T. Doherty-Welch Chair in Chemistry (A-0001).

■ REFERENCES

(1) Hearon, K.; Singhal, P.; Horn, J.; Small, W.; Olsovsky, C.; Maitland, K. C.; Wilson, T. S.; Maitland, D. J. *Polym. Rev.* **2013**, *53* (1), 41−75.

(2) Yakacki, C.; Gall, K. Shape-Memory Polymers for Biomedical Applications. In *Advances in Polymer Science*: Springer: Berlin and Heidelberg, Germany: 2010; Vol. *226*, pp 147−175.

(3) Yakacki, C. M.; Shandas, R.; Safranski, D.; Ortega, A. M.; Sassaman, K.; Gall, K. *Adv. Funct. Mater.* **2008**, *18* (16), 2428−2435.

(4) Di Prima, M. A.; Lesniewski, M.; Gall, K.; McDowell, D. L.; Sanderson, T.; Campbell, D. *Smart Mater. Struct.* **2007**, *16* (6), 2330−2340.

(5) Fabrizio, Q.; Loredana, S.; Anna, S. E. *Mater. Lett.* **2012**, *69* (0), 20−23.

(6) Small, I. V. W.; Singhal, P.; Wilson, T. S.; Maitland, D. J. *J. Mater. Chem.* **2010**, *20* (17), 3356−3366.

(7) Rodriguez, J. N.; Yu, Y.-J.; Miller, M. W.; Wilson, T. S.; Hartman, J.; Clubb, F. J.; Gentry, B.; Maitland, D. J. *Ann. Biomed. Eng.* **2012**, *40* (4), 883−897.

(8) Singhal, P.; Rodriguez, J. N.; Small, W.; Eagleston, S.; Van de Water, J.; Maitland, D. J.; Wilson, T. S. *J. Polym. Sci., Part B: Polym. Phys.* **2012**, *50* (10), 724−737.

(9) Ware, T.; Simon, D.; Arreaga-Salas, D. E.; Reeder, J.; Rennaker, R.; Keefer, E. W.; Voit, W. *Adv. Funct. Mater.* **2012**, *22* (16), 3470−3479.

(10) Ware, T.; Hearon, K.; Lonnecker, A.; Wooley, K. L.; Maitland, D. J.; Voit, W. *Macromolecules* **2012**, *45* (2), 1062−1069.

(11) Yu, Y.-J.; Hearon, K.; Wilson, T. S.; Maitland, D. J. *Smart Mater. Struct.* **2011**, *20* (085010), No. 085010.

(12) Xie, T. *Nature* **2010**, *464* (7286), 267−270.

(13) Behl, M.; Lendlein, A. *Mater. Today* **2007**, *10* (4), 20−28.

(14) Liu, C.; Qin, H.; Mather, P. T. *J. Mater. Chem.* **2007**, *17*, 1543−1558.

(15) Volk, B. L.; Dimitris, C. L.; Maitland, D. J. *Smart Mater. Struct.* **2011**, *20* (9), 094004.

(16) Lendlein, A.; Behl, M.; Hiebl, B.; Wischke, C. *Exp. Rev. Med. Dev.* **2010**, *7* (3), 357−379.

(17) Schulze, U.; Majumder, P. S.; Heinrich, G.; Stephan, M.; Gohs, U. *Macromol. Mater. Eng.* **2008**, *293* (8), 692−699.

(18) Bracco, P.; Brunella, V.; Luda, M. P.; Zanetti, M.; Costa, L. *Polymer* **2005**, *46* (24), 10648−10657.

(19) Vijayabaskar, V.; Bhattacharya, S.; Tikku, V. K.; Bhowmick, A. K. *Radiat. Phys. Chem.* **2004**, *71* (5), 1045−1058.

(20) Hearon, K.; Smith, S. E.; Maher, C. A.; Wilson, T. S.; Maitland, D. J. *Radiat. Phys. Chem.* **2013**, *83* (0), 111−121.

(21) Ortega, A. M.; Yakacki, C. M.; Dixon, S. A.; Likos, R.; Greenberg, A. R.; Gall, K. *Soft Matter* **2012**, *8* (28), 3381−3392.

(22) Pillai, S. D. Electron Beam Pasteurization as an Intervention in Poultry Processing Issues and Applications. In *Multimedia-Presentations*: National Center for Electron Beam Research, Texas A&M University: College Station, TX, 2012.

(23) Hearon, K.; Gall, K.; Ware, T.; Maitland, D. J.; Bearinger, J. P.; Wilson, T. S. *J. Appl. Polym. Sci.* **2011**, *121* (1), 144−153.

(24) Hearon, K.; Nash, L. D.; Volk, B. L.; Ware, T.; Lewicki, J. P.; Voit, W. E.; Wilson, T. S.; Maitland, D. J. *Macromol. Chem. Phys.* **2012**, *214* (11), 1258−1272.

(25) Hill, D. J. T.; O'Donnell, J. H.; Perera, M. C. S.; Pomery, P. J.; Smetsers, P. *J. Appl. Polym. Sci.* **1995**, *57* (10), 1155−1171.

(26) Shultz, A. R.; Bovey, F. A. *J. Polym. Sci.* **1956**, *XXII* (102), 485−494.

(27) Bovey, F. A.; Kolthoff, I. M. *Chem. Rev.* **1948**, *42* (3), 491−525.

(28) Julich-Gruner, K. K.; Löwenberg, C.; Neffe, A. T.; Behl, M.; Lendlein, A. *Macromol. Chem. Phys.* **2013**, *214* (5), 527−536.

(29) Zhu, G.; Liang, G.; Xu, Q.; Yu, Q. *J. Appl. Polym. Sci.* **2003**, *90* (6), 1589−1595.

(30) Safranski, D. L.; Gall, K. *Polymer* **2008**, *49* (20), 4446−4455.

(31) Charlesby, A.; Pinner, S. H. *Proc. R. Soc. London, Ser. A: Math. Phys. Sci.* **1959**, *249* (1258), 367−386.

(32) Ware, T.; Voit, W.; Gall, K. *Radiat. Phys. Chem.* **2010**, *79* (4), 446−453.

(33) James, H. M.; Guth, E. *J. Chem. Phys.* **1943**, *11* (10), 455.

(34) Gall, K.; Yakacki, C. M.; Liu, Y.; Shandas, R.; Willett, N.; Anseth, K. S. *J. Biomed. Mater. Res., Part A* **2005**, *73A* (3), 339−348.

(35) James, H. M.; Guth, E. *J. Chem. Phys.* **1947**, *15* (9), 669−683.
(36) Wilson, T. S.; Bearinger, J. P.; Herberg, J. L.; J. E., M., III; Wright, W. J.; Evans, C. L.; Maitland, D. J. *J. Appl. Polym. Sci.* **2007**, *106* (1), 540−551.
(37) Hedrick, J. L.; Mohanty, D. K.; Johnson, B. C.; Viswanathan, R.; Hinkley, J. A.; McGrath, J. E. *J. Polym. Sci., Part A: Polym. Chem.* **1986**, *24* (2), 287−300.
(38) Flory; J., P. *Principles of polymer chemistry*. Cornell University Press: Ithaca, NY, 1953.